



HAL
open science

INELASTIC PROPERTIES OF ICE I_h AT LOW TEMPERATURES AND HIGH PRESSURES

S. Kirby, W. Durham, M. Beeman, H. Heard, M. Daley

► **To cite this version:**

S. Kirby, W. Durham, M. Beeman, H. Heard, M. Daley. INELASTIC PROPERTIES OF ICE I_h AT LOW TEMPERATURES AND HIGH PRESSURES. *Journal de Physique Colloques*, 1987, 48 (C1), pp.C1-227-C1-232. 10.1051/jphyscol:1987131 . jpa-00226277

HAL Id: jpa-00226277

<https://hal.science/jpa-00226277>

Submitted on 4 Feb 2008

HAL is a multi-disciplinary open access archive for the deposit and dissemination of scientific research documents, whether they are published or not. The documents may come from teaching and research institutions in France or abroad, or from public or private research centers.

L'archive ouverte pluridisciplinaire **HAL**, est destinée au dépôt et à la diffusion de documents scientifiques de niveau recherche, publiés ou non, émanant des établissements d'enseignement et de recherche français ou étrangers, des laboratoires publics ou privés.

INELASTIC PROPERTIES OF ICE I_h AT LOW TEMPERATURES AND HIGH PRESSURES

S.H. KIRBY, W.B. DURHAM*, M.L. BEEMAN**, H.C. HEARD* and
M.A. DALEY

U.S. Geological Survey, 345 Middle Road MS 977, Menlo Park,
CA 94025, U.S.A.

*Lawrence Livermore National Laboratory, Livermore, CA 94550,
U.S.A.

**Dept. Materials Science, Cornell University; Ithaca,
NY 14853, U.S.A.

Résumé - Le but de notre programme de recherche est d'étudier le comportement rhéologique de glaces soumises aux mêmes conditions que celles existant à l'intérieur de satellites des planètes extérieures afin de connaître leurs lois de déformation. Pour cela, nous avons effectué 100 essais de compression à vitesse de déformation constante pour des pressions allant jusqu'à 500 MPa et pour des températures aussi basses que 77 K. Pour $P > 30$ MPa, la glace I_h se fracture par instabilité de cisaillement produisant des fautes dans la direction du maximum de contrainte de cisaillement et la contrainte de fissuration est indépendante de la pression. Ce comportement inhabituel peut-être associé à des transformations de phases localisées dans les zones de cisaillement.

La résistance en régime stationnaire suit des lois rhéologiques thermiquement activées décrites par des lois de puissance, avec différents paramètres d'écoulement dépendant des gammes de températures étudiées. Les lois d'écoulement seront discutées en relation avec les divers mécanismes de déformation déduits des microstructures observées optiquement et en comparaison avec d'autres travaux.

Abstract - The aim of our research programme is to explore the rheological behavior of H_2O ices under conditions appropriate to the interiors of the icy satellites of the outer planets in order to give insight into their deformation. To this end, we have performed over 100 constant-strain-rate compression tests at pressures to 500 MPa and temperatures as low as 77 K.

At $P > 30$ MPa, ice I_h fails by a shear instability producing faults in the maximum shear stress orientation and failure strength typically is independent of pressure. This unusual faulting behavior is thought to be connected with phase transformations localized in the shear zones. The steady-state strength follows rheological laws of the thermally-activated power-law type, with different flow law parameters depending on the range of test temperatures. The flow laws will be discussed with reference to the operating deformation mechanisms as deduced from optical-scale microstructures and comparison with other work.

1. Introduction - Ice flows plastically under the force of gravity on a large scale on the Earth's surface and interest in this natural phenomenon has motivated a long history of research on ice rheology at the high temperature and low pressures, conditions appropriate to the natural terrestrial environment. It is now arguably the best characterized crystalline Earth material as far as its rheology under natural conditions. H_2O ices also exist in abundance in the outer solar system and of particular interest is the fact that the H_2O ices exist in that exotic environment at temperatures as low as 35 K and pressures as high as several GPa [1]. Not only are these conditions far removed from previous experimental and terrestrial field experience, other high-pressure forms of ice are expected to be stable in the interiors of these icy moons and planets. Many internal processes

connected with the thermomechanical evolution of these bodies involve the fracture and flow properties of H₂O ice and hence we were motivated to explore the inelastic properties of this compound at temperatures and pressures far removed from previous work in order to provide some of the tools for interpreting the surface features that stem from these internal processes. A companion paper [2] reports the flow properties of ice II, III and V. This paper first explores the failure processes that dominate at laboratory time scales at temperatures below about 165 K. Second, we review the important effects of temperature and deformation rates on the steady-state plastic strength of polycrystalline ice I_h and demonstrate that the rheological laws determined at high temperatures for ice are an inadequate description of the flow behavior at lower temperatures. Lastly, we describe some preliminary optical thin section textures and structures that are revealing of the operating plastic deformation mechanisms.

2. Experimental details.- Clear isotropic polycrystalline aggregates of ice I_h were prepared by a standard molding technique [4], resulting in a polygonal grain texture, uniform grain size of 700 μm (linear intercept method [3]), and sample size 25.4 mm diameter and 62 mm length. The specimens were jacketed in indium and shortened at constant rates in a high-pressure gas apparatus designed to deform ice at low temperatures [4]. The differential stress $\sigma = \sigma_1 - \sigma_3$ (σ_1 and σ_3 are the maximum and minimum principal compressive stresses) and engineering strain ϵ were calculated from the force and displacement transducer records and the resulting effects of strain rate $\dot{\epsilon}$, absolute temperature T, and confining pressure P_C on the stress-strain curves were determined. See our earlier publications [4, 13] for further details.

3. Experimental results.- 3.1. Pressure effects T at ≤ 165 K.- Four failure processes are important at low temperatures: (1) Axial splitting at confining pressures near 0.1 MPa. This process involves the production, growth and coalescence of tensile microcracks oriented parallel to the specimen compression axis and normal to the least principal compressive stress and is a common mode of failure of brittle materials under near-uniaxial compression conditions [6]. (2) Brittle shear fracture on inclined faults where the failure strength σ_f increases steeply with increasing pressure (see Fig. 1). Again, this is a very

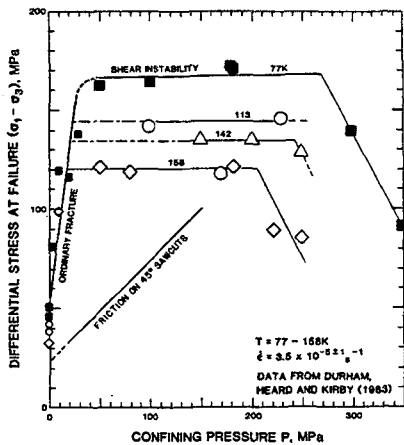


Fig. 1.- Failure strengths σ_f of ice I_h at low temperatures (T < 165 K) and elevated pressures [from unpublished data and 4].

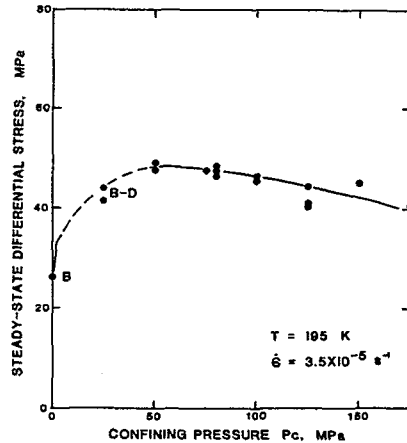


Fig. 2.- Variation of the strength of ice with confining pressure at T = 195 K.

common failure mode of rocks and ceramics at elevated confining pressure [6] and is thought to develop from the production, growth and interaction of tensile microcracks [7]. Failure strength is relatively insensitive to temperature and strain rate [4]. (3) Frictional sliding along preexisting fractures. After a shear

fault has formed, the resistance to frictional sliding is less than that required to form a fault (Fig. 1) and hence subsequent deformation takes place by sliding [8]. Separate tests on samples with precut and ground artificial faults indicate that ice I_h displays a frictional law of the form

$$\tau_f = 8.5 \text{ MPa} + 0.2 \sigma_n \text{ (MPa)} \quad (1)$$

where τ_f is the shear stress necessary to overcome static friction and σ_n is the normal stress on the sliding surface at the time that sliding occurs [9]. Friction in ice at these conditions is unstable, producing rapid stress drops that can take place repeatedly upon reloading if the jacket does not rupture. The sliding strength generally increases with event number, reaching an apparent plateau after several cycles. The friction law of eq. (1) is relatively insensitive to temperatures over the range 77 to 115 K and sliding velocities ranging from 3×10^{-4} to $3 \times 10^{-2} \text{ mm s}^{-1}$ and normal stresses from 20 to 250 MPa. The micromechanical mechanisms controlling ice friction under these conditions are unknown. (4) High-pressure shear instability. Above a confining pressure of 30 MPa at $T < 165 \text{ K}$, ice exhibits an unusual form of shear failure. It is unusual because pressure does not increase the failure strength σ_f ; σ_f is either independent of P_c or σ_f decreases with increasing P_c (Fig. 1). These faults form in the maximum shear stress orientation (45° to the compression direction) and in the one test in which the jacket did not leak after failure occurred, a subsequent failure occurred at about the same σ_f , indicating that cohesion was not reduced during the first event, in contrast with ordinary shear fracture. Kirby [10] proposes that this shear instability is connected with the localization in the fault of a polymorphic phase change to ice II and cites an example of another non-metallic compound that exhibited nearly identical behavior.

3.2. Pressure effects at $T \geq 165 \text{ K}$.- At higher temperatures, ice I_h exhibits a typical brittle-ductile transition with increasing confining pressure which depends upon temperature and strain rate. At pressures less than about 10 MPa at 195 K, ordinary shear fracture occurs with σ_f increasing steeply with increasing P_c (Fig. 2). At intermediate pressures, transitional brittle-ductile behavior occurs. At $P_c > 50 \text{ MPa}$, the samples deform by essentially homogeneous plastic deformation and the steady-state strength σ_s (explained below) slightly decreases with increasing P_c . This pressure effect is consistent with a negative activation volume for creep of $-13 \times 10^{-6} \text{ m}^3/\text{mole}$ (see flow law discussion below).

3.3. Microstructural interpretation of the stress strain curves.- All of the tests in the ductile regime exhibit linear quasi-elastic behavior at low stresses, followed by macroscopic yield at σ_y , a peak in the stress-strain curve at σ_m followed by strain softening and then steady-state strength σ_s to strains of about 0.20 where barreling of the samples becomes too pronounced to make meaningful measurements of stress and strain. Thin sections of samples taken to various strains along a stress-strain curve at $T = 213 \text{ K}$, $\dot{\epsilon} = 3.5 \times 10^{-4} \text{ s}^{-1}$ and $P_c = 100 \text{ MPa}$ indicate the following evolution of inelastic processes: (A) At low strains where stresses are between σ_y and σ_m , samples show plastic deformation features in the original grains as indicated by variable extinction (optical orientation changes) in individual grains. (B) At strains just beyond σ_m , new recrystallized grains appear for the first time and no optical-scale evidence for plastic deformation in original or recrystallized grains is seen. (C) At strains sufficiently high that steady-state flow strength is attained, the recrystallized grain size stabilizes to values less than those observed in the strain-softening part of the stress-strain curve. There is no evidence for significant grain flattening at any stage of the stress-strain curve. We conclude that the strain-softening stages are associated with the onset of recrystallization and that the attainment of steady-state flow is connected with the stabilization of recrystallized grain size. In the discussion below, we explore the systematic effects of T , $\dot{\epsilon}$ and P_c on σ_s .

3.4. Effects of temperature, strain rate and pressure on steady-state strength.- For the purposes of discussion, we plot the steady-state strengths on a $\log \sigma_s$ versus $1/T(K)$ basis for four different strain rates (Fig. 3). If ice I_h follows a flow law of the general form

$$\dot{\epsilon} = A\sigma^n \exp(-Q^*/RT) \tag{2}$$

then the data should plot linearly with slopes equal to $Q^*/2.303 nR$. In equation (2), A, n and Q^* are material constants that depend upon deformation mechanism. Q^* is the activation energy for steady-state flow which contains an effect of pressure P: $Q^* = H^* + PV^*$ where H^* is the activation enthalpy and V^* is the activation volume. The data indicate three distinct regimes of flow: (1) Regime A at the highest temperatures which displays the largest effect of temperature on σ_s . In Figure 3 we also plot the uniaxial σ_s data of Mellor and Cole [11] which clearly shows that our flow data converges with data collected for glaciological purposes at higher temperature and room pressure. The least-squares fits to this data set (Table 1) indicate $n = 4.0 \pm 0.6$ and $Q^* = 91 + 2 \text{ kJ mol}^{-1}$, values very close to those reported by others in this temperature range (see review by Weertman [12]). Samples deformed in this regime are unusually clear and thin sections cut from them show evidence for grain boundary mobility in the form of grain growth and grain boundary bowing. (2) Regime B in which recrystallized grains are polygonal in shape and neither grain shape changes nor internal plastic deformation features are observed at the optical scale in the deformed samples. Although the stress exponent n is essentially the same as in regime A, Q^* is markedly lower at $61 \pm 2 \text{ kJ mol}^{-1}$. (3) Regime C, in which partial recrystallization has occurred but evidently has not kept pace with internal deformation, judging from the plastic deformation features (bending and kinking) that are prominent in many of the grains. The $n = 4.7 \pm 0.2$ and $Q^* = 36 \pm 5 \text{ kJ mol}^{-1}$ are both significantly different than at higher temperatures and lower stresses. It should be emphasized that the flow-law parameters characterizing regime C are the least-well determined of

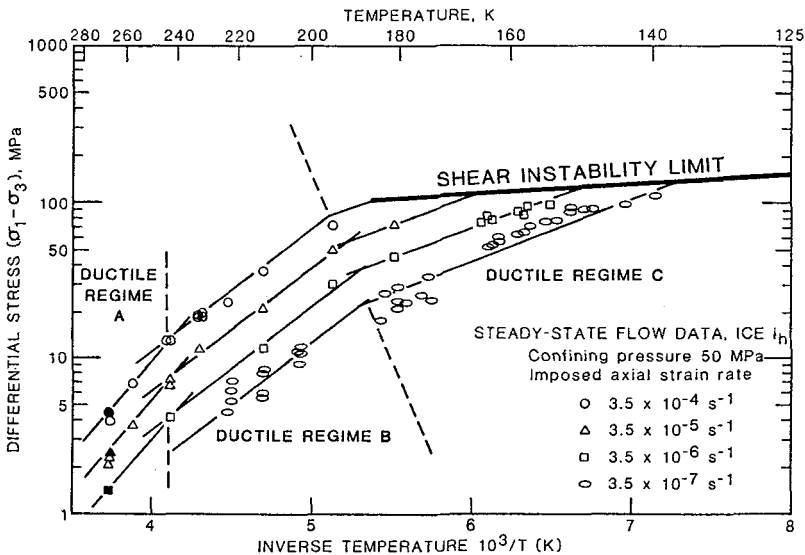


Fig. 3.- Variation of steady-state flow stress σ_s with temperature T at four different strain rates plotted on a $\log_{10} \sigma_s$ versus $1/T(K)$ basis. The interpolated data of Mellor and Cole [11] is shown as filled symbols. The slopes of the curves are proportional to the activation energy Q^* and the separation between the data at various strain rates reflects the stress exponent n. Note the different flow regimes that evidently reflect changes in deformation mechanisms.

the three because of the narrower strain rate range imposed by the high-pressure faulting instability and this flow law may be contaminated by subtle transitional behavior toward the faulting behavior.

Table 1. Flow law parameters for ice at a confining pressure of 50 MPa

Regime	$\log_{10} A$ [MPa ⁻ⁿ s ⁻¹]	n	Q*	V*
			[kJ mol ⁻¹]	[m ³ mol ⁻¹]
Ductile C Low T (\lesssim 195 K)	-2.8 \pm 0.6	4.7 \pm 0.3	36 \pm 5	--
Ductile B Intermediate T (~195-240 K)	5.10 \pm 0.03	4.0 \pm 0.1	61 \pm 2	-(13 \pm 3) \times 10 ⁻⁶
Ductile A High T (240-258 K)	11.8 \pm 0.4	4.0 \pm 0.6	91 \pm 2	--

4. Interpretation of the ductile flow regimes.- We have already reviewed in another paper [13] the probable deformation mechanisms that control the rheological laws displayed by ice I_h . Regime B is probably the best understood. The activation energy for creep $Q^* = 61 \pm 2$ kJ mol⁻¹ is nearly identical with that for molecular H₂O diffusion (66 ± 13 kJ mol⁻¹ [14]) and so is similar to many power law materials deformed at high temperature where dislocation recovery processes dominate [12, 15, 16]. Alternatively, a diffusion-controlled dislocation glide process may be operating [12, 18]. At higher temperatures, grain boundary processes evidently are involved since the transition in activation energies between regimes A and B do not occur in single-crystal tests [17, 18]. Liquid along grain boundaries that facilitates grain boundary migration and intergrain interactions has been frequently cited as contributing to the higher activation energy in this regime (see reviews in [17] and [18]). The evidence of enhanced grain-boundary migration in our samples is consistent with this interpretation. Regime C is more difficult to interpret. Samples deformed under these conditions show clear evidence for internal deformation, as we noted earlier in this paper. The higher n value and lower activation energy may be more indicative of strictly glide-controlled creep. Alternatively, the apparent flow-law parameters may be merely transitional to those appropriate to lower temperatures which we could not explore because our tests were truncated by the shear instability phenomenon. The lack of detailed knowledge of dislocation and point defect properties at these low temperatures obviously hampers our understanding of the flow properties of ice I_h at low temperatures.

5. Conclusions.- Ice I_h displays a rich variety of inelastic behavior at low to intermediate temperatures, behavior that stems from a range of deformation processes that are poorly understood. These exploratory experiments are only a beginning in trying to better understand the rheology of this intriguing material at low temperatures.

Acknowledgments.- We thank Carl Boro and Laura Stern for their technical assistance in apparatus construction and maintenance and sample preparation. This work was performed under contract W-7405-ENG-48 with NASA which we gratefully acknowledge. Beverly Monroe performed her usual magic in typing the manuscript.

References

- [1] Consolmagno, G.J., J. Phys. Chem. 87 (1983) 4204-4208.
- [2] Durham, W.B., Kirby, S.H., Heard, H.C. and Stern, L.A., Inelastic properties of several high pressure crystalline phases of H₂O: ices II, III and V, Journal de Physique, this volume.

- [3] Smith, C.S. and Guttman, L., *Trans. AIME* 197 (1953) 81-87.
- [4] Durham, W.B., Heard H.C. and Kirby, S.H., *J. Geophys. Res.* 88 (Supplement) (1983) B377-B392.
- [5] Kirby, S.H. and Daley, M.K., *J. Glaciology* 30 (1984) 248-250.
- [6] Paterson, M.S., *Rock Deformation - The Brittle Field* (Springer-Verlag, Berlin).
- [7] Brace, W.F., Paulding, B.W. and Scholz, C., *J. Geophys. Res.* 71 (1966) 3939-3953.
- [8] Kirby, S.H., *Tectonophysics* 119 (1985) 1-27.
- [9] Beeman, M., Durham, W.B. and Kirby, S.H., *Friction of ice*, *J. Geophys. Res.* (1987), in press.
- [10] Kirby, S.H., *Localized polymorphic phase transformations in high pressure faults and applications to the physical mechanism of deep earthquakes*, *J. Geophys. Res.* (Special Issue of Deep Earthquakes) (1987), in press.
- [11] Mellor, M. and Cole, D.M., *Cold Regions Science and Technology* 5 (1982) 201-219.
Mellor, M., and Cole, D.M., *Cold Regions Science and Technology* 6 (1983) 207-230.
- [12] Weertman, J., *Ann. Rev. Earth Planet. Sci.* (1983) 215-240.
- [13] Kirby, S.H., Durham, W.B. and Heard, H.C., in "Ices in the solar system", J. Klinger *et al.*, eds., (D. Reidel Publishing, Dordrecht, Holland) 1985, p. 89-107.
- [14] Delibaltas, P., Dengel, O., Helmreich, D., Riehl, N. and Simon, H., *Phys. Kondens. Materie* 5 (1966) 166-170.
- [15] Frost, H.J. and Ashby, M.F., *Deformation-Mechanism Maps*, (Pergamon Press, Oxford) (1982), 166 p.
- [16] Duval, Paul, Ashby, M.F. and Anderman, I., *J. Phys. Chem.* 87 (1983) 4066-4074.
- [17] Homer, D.R. and Glen, J.W., *J. Glaciology* 21 (1978) 429-444.
- [18] Jones, S.J. and Brunet, J.-G., *J. Glaciology* 21 (1978) 445-456.